

Article

Structurally Rigid (8-(Arylimino)-5,6,7-trihydroquinolin-2-yl)-methyl Acetate Cobalt Complex Catalysts for Isoprene Polymerization with High Activity and *cis*-1,4 Selectivity

Nighat Yousuf^{1,2,3}, Yanping Ma^{1,*} , Qaiser Mahmood^{2,*}, Wenjuan Zhang^{4,*}, Ming Liu^{1,3} , Rongyan Yuan² and Wen-Hua Sun^{1,2,3,*} 

- ¹ Key Laboratory of Engineering Plastics and Beijing National Laboratory for Molecular Science, Institute of Chemistry, Chinese Academy of Sciences, Beijing 100190, China; nigiyousuf@iccas.ac.cn (N.Y.); liuming@iccas.ac.cn (M.L.)
- ² Chemistry and Chemical Engineering Guangdong Laboratory, Shantou 515031, China; 1020210212@glut.edu.cn
- ³ CAS Research/Education Center for Excellence in Molecular Sciences and International School, University of Chinese Academy of Sciences, Beijing 100049, China
- ⁴ Beijing Key Laboratory of Clothing Materials R&D and Assessment, School of Materials Science and Engineering, Beijing Institute of Fashion Technology, Beijing 100029, China
- * Correspondence: myanping@iccas.ac.cn (Y.M.); qaiser@cclab.com.cn (Q.M.); zhangwj@bift.edu.cn (W.Z.); whsun@iccas.ac.cn (W.-H.S.); Tel.: +86-1062557955 (Y.M. & W.-H.S.)

Abstract: A series of cobalt complexes bearing (8-(arylimino)-5,6,7-trihydroquinolin-2-yl)methyl acetate ligand framework were prepared using a one-pot synthesis method. These complexes were then extensively investigated for their catalytic performance in isoprene polymerization. In addition to the complexes being characterized via FT-IR spectrum and elemental analysis, the molecular structure of Co1 and Co5 was determined via X-ray diffraction analysis. The analysis revealed a chloride-bridged centrosymmetric binuclear species in which each cobalt center exhibited a distorted square pyramidal geometry. Among the prepared complexes, Co1 demonstrated the highest catalytic activity of 1.37×10^5 g (mol of Co)⁻¹(h)⁻¹, achieving complete monomer conversion and resultant polyisoprene showed high molecular weight ($M_n \geq 2.6 \times 10^5$ g/mol). All of the complexes showed preference for the *cis*-1,4 configuration ranging from 65% to 72%, while the 3,4 monomer insertion units constituted between 27% and 34% of the polymer structure. Moreover, extensive investigations were conducted to assess the impact of reaction parameters and ligand properties on the catalytic activities and microstructural characteristics of the resulting polymer.

Keywords: Coordination-insertion polymerization; isoprene; polyisoprene; cobalt catalysts; *cis*-1,4 microstructure; 3,4 microstructure



Citation: Yousuf, N.; Ma, Y.; Mahmood, Q.; Zhang, W.; Liu, M.; Yuan, R.; Sun, W.-H. Structurally Rigid (8-(Arylimino)-5,6,7-trihydroquinolin-2-yl)-methyl Acetate Cobalt Complex Catalysts for Isoprene Polymerization with High Activity and *cis*-1,4 Selectivity. *Catalysts* **2023**, *13*, 1120. <https://doi.org/10.3390/catal13071120>

Academic Editor: Ken-ichi Fujita

Received: 22 June 2023

Revised: 13 July 2023

Accepted: 15 July 2023

Published: 18 July 2023



Copyright: © 2023 by the authors. Licensee MDPI, Basel, Switzerland. This article is an open access article distributed under the terms and conditions of the Creative Commons Attribution (CC BY) license (<https://creativecommons.org/licenses/by/4.0/>).

1. Introduction

Polyisoprene, as a viable alternative to natural rubber, possesses exceptional thermal, mechanical and physical properties, making it highly suitable for various industries such as rubber manufacturing, shape memory technology, and medicinal applications [1,2]. Among various significant attributes, the mechanical properties of polyisoprene heavily rely on the intricate microstructure of the polymer, which is determined by the type of isoprene enchainment within the polymer chain. There are four predominant types of isoprene enchainments: *cis*-1,4, *trans*-1,4, 3,4 and the less commonly observed 1,2 isoprene configuration. The quantity and nature of these monomer enchainments play a crucial role in determining the desired properties and applications of polyisoprene [3,4]. Highly *trans*-1,4 polyisoprene exhibits enhanced crystallinity and toughness [5]. Conversely, the presence of *cis*-1,4 enchainment imparts remarkable flexibility and low crystallinity to the

material [6], rendering it particularly desirable as a primary component in bulk tire production due to its exceptional elastomeric properties. Generally, the high rolling resistance of *cis*-1,4 polyisoprene-based tires makes them unsuitable for use in harsh environment [7]. To address this issue, incorporation of 3,4 units into *cis*-1,4 polyisoprene chains is an excellent strategy to reduce rolling resistance while maintaining high wet-skid resistance and wear resistance [8]. During the past few decades, numerous catalysts have been suggested to achieve highly selective synthesis of polyisoprene. However, most successful developments have been achieved by using coordination-insertion polymerization catalysts. Over the past 60 years, isoprene polymerization has primarily relied on early transition metal catalysts or conventional Ziegler–Natta catalysts [9,10]. However, recent advancements in late transition metal-catalyzed polymerization have brought about exciting developments in the field. The discovery of α -diimine-Ni(II)/Pd(II) complexes in 1995 [11,12], followed by bis(imino)pyridine-Fe(II)/Co(II) complexes for olefin polymerization [13,14], has attracted significant interest among both academic researchers and the industrial community. These breakthroughs have also stimulated notable progress in late-transition metal catalysts specifically designed for isoprene polymerization [3,4,15]. One of the key advantages of these complexes is their well-defined molecular structures, which play a vital role in controlling monomer enchainment, molecular weights, and molecular weight distributions, enabling the production of polymers with desired mechanical and physical properties. Iron and cobalt catalysts have become the preferred choices for isoprene polymerization due to advantages such as low cost, ready availability, high stability, moisture and air stability in most cases, ease of preparation, and demonstrated high activity and selectivity [16–19]. Both bidentate and tridentate ligand chelated iron and cobalt complexes have been explored, with bidentate ligand-metal complex catalysts demonstrating superior polymerization activity and molecular weights [20–26]. Bidentate iminopyridine-iron complex with high catalytic activity and high stereoselectivity for *cis*-1,4 and *trans*-1,4 microstructure was initially reported for isoprene polymerization [16], and subsequently, extensive structural modifications into this ligand framework have been explored, particularly for iron complexes [27–30]. However, there have been limited reports on iminopyridine-cobalt complexes due to their low polymerization activities. Recently, Chen et al. reported on iminopyridine-based cobalt complexes (A, Chart 1) with polymerization activity up to $8.3 \times 10^4 \text{ g (mol of Co)}^{-1}(\text{h})^{-1}$, producing polyisoprene with low molecular weights up to 1.8 kg/mol [31]. Later, Wang et al. investigated the influence of fluorine substituents on iminopyridine-cobalt complexes (B, Chart 1) and achieved polymerization activity up to $2.6 \times 10^4 \text{ g (mol of Co)}^{-1}(\text{h})^{-1}$, yielding polyisoprene with moderate-to-high molecular weight [32]. Recently, our group employed π -conjugated naphthalenyl-substituted iminopyridine-cobalt complexes (C, Chart 1) for isoprene polymerization, achieving high activity up to $3.2 \times 10^5 \text{ g (mol of Co)}^{-1}(\text{h})^{-1}$ and high selectivity for 1,4-polyisoprene [33]. Apart from variations in catalyst structure, reaction parameters, especially the type of co-catalyst, have significant influence on the polymerization rate and polymer properties [34–36].

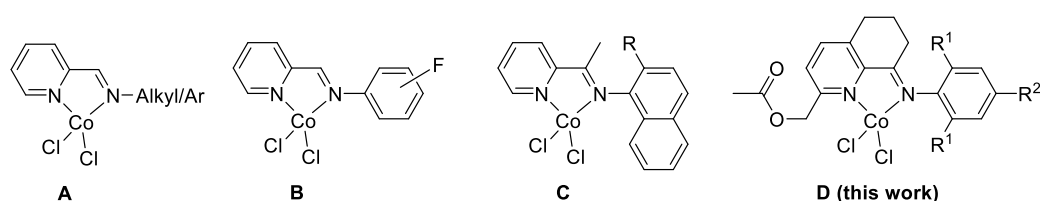


Chart 1. Iminopyridine-cobalt complexes previously studied for isoprene polymerization (A–C) along with prepared cobalt complexes (D) in this work.

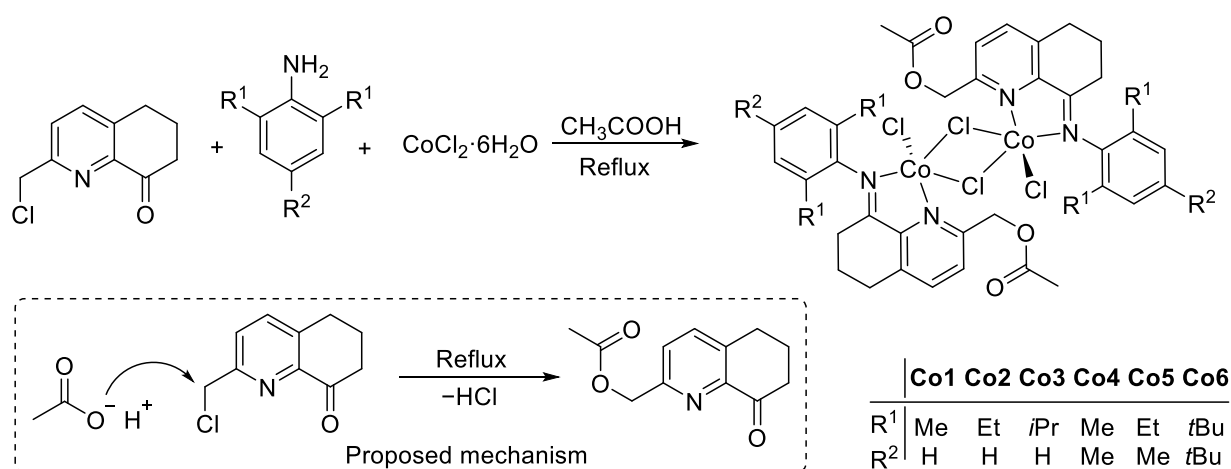
In recent years, our research group has prepared a series of nickel complexes based on *N*-(2-alkyl-5,6,7-trihydroquinolin-8-ylidene) arylimines for ethylene polymerization [37–42]. We observed that the incorporation of a carbocyclic ring into the iminopyridine-nickel complexes positively impacts the performance of ethylene polymerization, particularly

polymerization activity. Motivated by this observation, we hypothesized that incorporating a carbocyclic ring into the iminopyridine-cobalt complexes would aid in controlling monomer enchainment and further enhance the polymerization behavior of these catalysts. Herein, a series of cobalt complex catalysts based on (8-(arylimino)-5,6,7-trihydroquinolin-2-yl)methyl acetate ligands was prepared and their performance in isoprene polymerization was investigated. Isoprene polymerization experiments were extensively conducted to establish a clear structure–activity relationship. The significant influence of reaction conditions on the polymerization being recognized, the various reaction parameters, including the type and amount of co-catalyst, reaction temperature, run time, and catalyst loading, were systematically examined. By systematically studying these factors, we aimed to gain insights into their impact on the polymerization process and ultimately optimize the catalyst performance for isoprene polymerization.

2. Results and Discussion

2.1. Synthesis and Characterization of Cobalt Complexes (Co1–Co6)

Following the established procedure [29,43], a one-pot synthesis method was employed to prepare (8-(arylimino)-5,6,7-trihydroquinolin-2-yl)methyl acetate-cobalt dichloride complexes (where aryl = 2,6-Me₂C₆H₃ for **Co1**), 2,6-Et₂C₆H₃ for **Co2**, 2,6-*i*Pr₂C₆H₃ for **Co3**, 2,4,6-Me₃C₆H₂ for **Co4**, 2,6-Et₂-4-MeC₆H₂ for **Co5** and 2,4,6-*t*Bu₃C₆H₂ for **Co6**). The reaction involved refluxing 2-chloromethyl-5,6,7-trihydroquinolin-8-one, the corresponding aniline, and CoCl₂·6H₂O in acetic acid for 7 h. This synthetic procedure generated the desired cobalt complexes at high yields, as depicted in Scheme 1. Generally, the one-pot synthetic approach of complexes offered several advantageous, such as elimination of the need for purification and isolation of ligands. However, this approach can sometimes lead to unexpected reactions due to the use of harsh conditions such as high temperatures (120 °C) and acetic acid as the solvent [40]. Thus, in the synthesis of the desired complexes, an unexpected reaction occurred, leading to the incorporation of a methyl acetate functionality at the ortho position of the pyridine ring instead of anticipated chloro methyl group. This observation was confirmed via single-crystal X-ray diffraction analysis and elemental compositions. It is proposed that at elevated temperatures, acetic acid, used as the solvent, displaced the chloro group with an acetyl group, ultimately leading to the incorporation of a methyl acetate functionality at the ortho position of the pyridine ring. A mechanism for this unexpected reaction is proposed in Scheme 1. All synthesized complexes were thoroughly characterized using Fourier transform infrared (FT-IR) spectra and elemental analysis. Additionally, the molecular structures of two complexes, **Co1** and **Co5**, were examined via single-crystal X-ray diffraction analysis.



Scheme 1. Synthesis of cobalt (II) complexes and the possible mechanism of the incorporation of the methyl acetate group.

The elemental analysis data provided confirmation of the structural integrity of the complexes depicted in Scheme 1. In the FT-IR spectra, the characteristic stretching vibrations of the C=N_{imine} bonds within these complexes were observed in the range of 1619–1647 cm⁻¹. Upon comparison of these wave numbers with those of structurally related non-coordinated ligands reported in the literature [37,41,44], a noticeable shift of approximately 20 cm⁻¹ towards lower values was observed, indicating coordination of the cobalt metal with the ligand structure. These findings align with previous reports on analogous cobalt complexes [31–33]. Moreover, the stretching vibrations of carbonyl groups were observed at approximately 1740 cm⁻¹, which confirms the presence of methyl acetate functionality within the ligand structure.

Single crystals of **Co1** and **Co5**, suitable for X-ray determinations, were grown via the slow diffusion of *n*-hexane into a solution of the corresponding complexes in dichloromethane at ambient temperature. The molecular structures of both complexes, displayed in Figure 1, exhibit a chloride-bridged centrosymmetric binuclear species; thus, the discussion will focus on both complexes together. In this dimeric arrangement, each cobalt center is coordinated by two sp² nitrogen atoms derived from the (8-(arylimino)-5,6,7-trihydroquinolin-2-yl)methyl acetate ligand. Additionally, one chloride ion bridges the cobalt centers while the remaining chloride ion acts as a monodentate ligand [40,45]. This coordination pattern is observed in both complexes. In the molecular structure of both complexes, the basal plane is formed from N_{pyridine}, N_{imine}, and the bridging chloride atoms (Cl2 and Cl2) while Cl1 occupies an axial position, resulting in a distorted square pyramidal geometry around the metal center. According to the data in Table 1, the bond distance between N_{pyridine} and the cobalt metal is slightly greater than the N_{imine}-cobalt bond distance [Co1–N1 = 2.172 (4) Å for **Co1**; 2.157 (3) Å for **Co5** vs. Co1–N2 = 2.056 (4) Å for **Co1**; 2.058 (3) Å for **Co5**, respectively], indicating a stronger coordination between N_{imine} and the metal center compared to N_{pyridine}. The N(1)–Co(1)–N(2) bite angles in each complex are similar, measuring 77.53° (**Co1**) and 77.90° (**Co5**), albeit considerably smaller than the three other angles [N1–Co1–Cl2, N2–Co1–Cl2, Cl2–Co1–Cl2] within the square plane. Moreover, the planes of the N-aryl rings are oriented almost perpendicular to the chelate ring plane. These structural characteristics have been previously reported in related metal complexes [40,45,46].

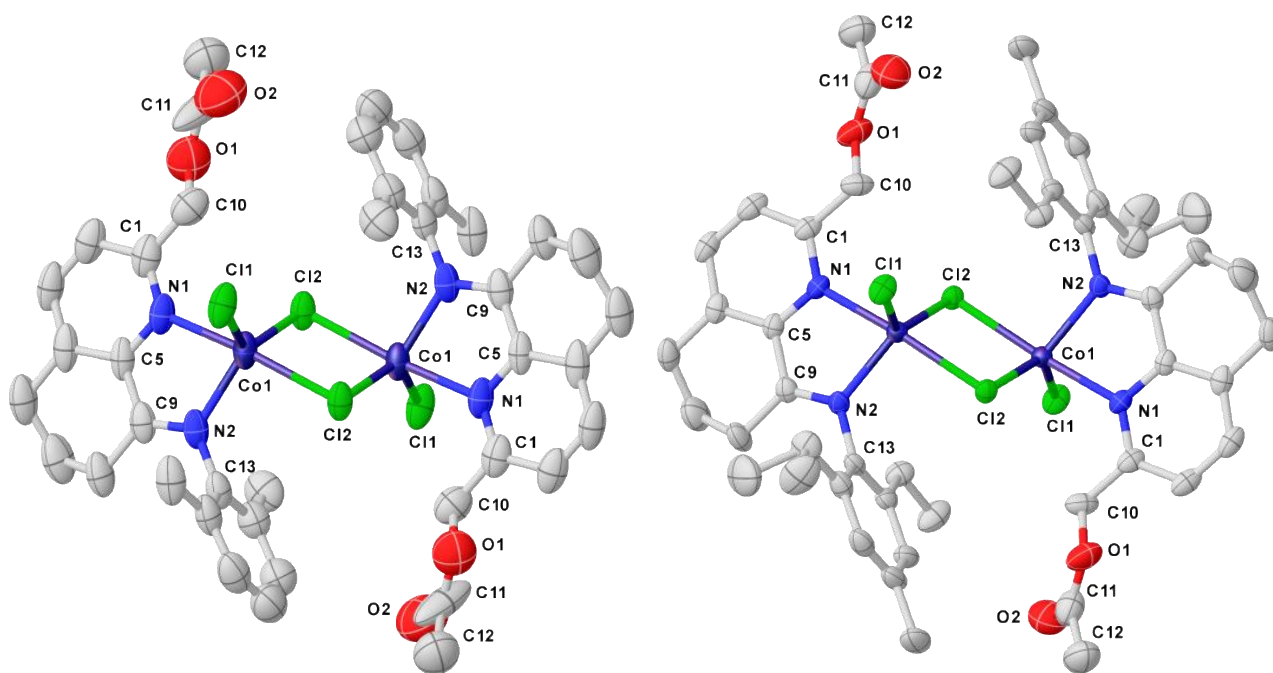


Figure 1. Molecular structure of **Co1** (left) and **Co5** (right) with thermal ellipsoids shown at 30% probability level. All hydrogen atoms are omitted for clarity.

Table 1. Selected bond lengths (Å) and bond angles (°) for **Co1** and **Co5**.

	Co1	Co5
Bond lengths (Å)		
Co1–N1	2.172 (4)	2.157 (3)
Co1–N2	2.056 (4)	2.058 (3)
Co1–Cl1	2.2812 (14)	2.2664 (11)
Co1–Cl2	2.3422 (12)	2.3420 (10)
N1–C1	1.321 (7)	1.334 (5)
N1–C5	1.345 (7)	1.357 (5)
N2–C9	1.292 (6)	1.295 (5)
N2–C13	1.440 (7)	1.441 (5)
Bond Angles (°)		
N1–Co1–Cl2	89.42 (10)	89.57 (9)
N1–Co1–N2	77.53 (16)	77.90 (13)
N2–Co1–Cl2	97.01 (11)	97.52 (10)
Cl2–Co1–Cl2	85.45 (3)	85.48 (3)
N2–Co1–Cl1	115.08 (11)	111.70 (10)
Cl1–Co1–Cl2	128.79 (6)	130.19 (5)
N1–Co1–Cl1	92.02 (11)	91.29 (9)

2.2. Isoprene Polymerization

2.2.1. Screening of Reaction Conditions Using **Co1** as Precatalyst

Previous studies have demonstrated the substantial impact of reaction parameters on the catalytic performance of complexes, particularly on the molecular weights and microstructure of the resulting polymers [25,34,45]. Consequently, we conducted a comprehensive screening of various reaction parameters, including reaction temperature, catalyst loading, and reaction time, as well as the type and quantity of co-catalyst employed. The aim was to identify the optimal reaction conditions that would serve as a reference point for evaluating the performance of all the synthesized complexes in isoprene polymerization.

The screening process for isoprene polymerization commenced with an evaluation of a suitable co-catalyst. The experiments were conducted using a fixed reaction time of 1 h in toluene solution (5 mL) at room temperature, utilizing complex **Co1** as the representative precatalyst. Three distinct alkylaluminum co-catalysts, namely methylaluminoxane (MAO), dimethylaluminum chloride (AlMe₂Cl), and trimethylaluminum (AlMe₃), were individually tested in combination with complex **Co1**. The polymerization results, as summarized in Table 2, revealed that **Co1** displayed activity only when paired with AlMe₂Cl (Al/Co ratio = 50), yielding a polymerization activity of $0.22 \times 10^5 \text{ g (mol of Co)}^{-1}(\text{h})^{-1}$ and producing polyisoprene with a molecular weight of $0.1 \times 10^5 \text{ g/mol}$. In contrast, MAO and AlMe₃ yielded only trace amounts of polymer. The disparity in polymerization activity can be attributed to the varying Lewis acidity of the co-catalysts, which plays a pivotal role in the activation of the catalysts. Therefore, AlMe₂Cl was identified as the optimal co-catalyst for subsequent investigations into isoprene polymerization.

Table 2. Selection of suitable co-catalyst for isoprene polymerization using **Co1** as the precatalyst ^a.

Entry	Co-Cat.	Al/Co	Conv. ^b (%)	Act. ^c	M_n ^d (10^5 , g/mol)	PDI ^d	Microstructure ^e		
							<i>cis</i> -1,4	<i>trans</i> -1,4	3,4
1	MAO	100	trace	-	-	-	-	-	-
2	AlMe ₃	50	trace	-	-	-	-	-	-
3	AlMe ₂ Cl	50	16	0.22	0.1	1.2	74	1	25
4	AlMe ₂ Cl	40	22	0.30	2.9	1.7	71	4	25
5	AlMe ₂ Cl	20	29	0.40	2.8	1.6	71	5	24
6	AlMe ₂ Cl	10	18	0.25	2.6	2.3	70	2	28

^a General conditions: catalyst **Co1** (10 μmol); isoprene 2 mL (20 mmol); IP/Co (2000); 5 mL toluene, reaction time 1 h, reaction temperature 25 °C, ^b isolated yield; ^c $10^5 \text{ g (mol of Co)}^{-1}(\text{h})^{-1}$; ^d determined via GPC, ^e selectivity given in mol%, determined via ¹H and ¹³C NMR spectra.

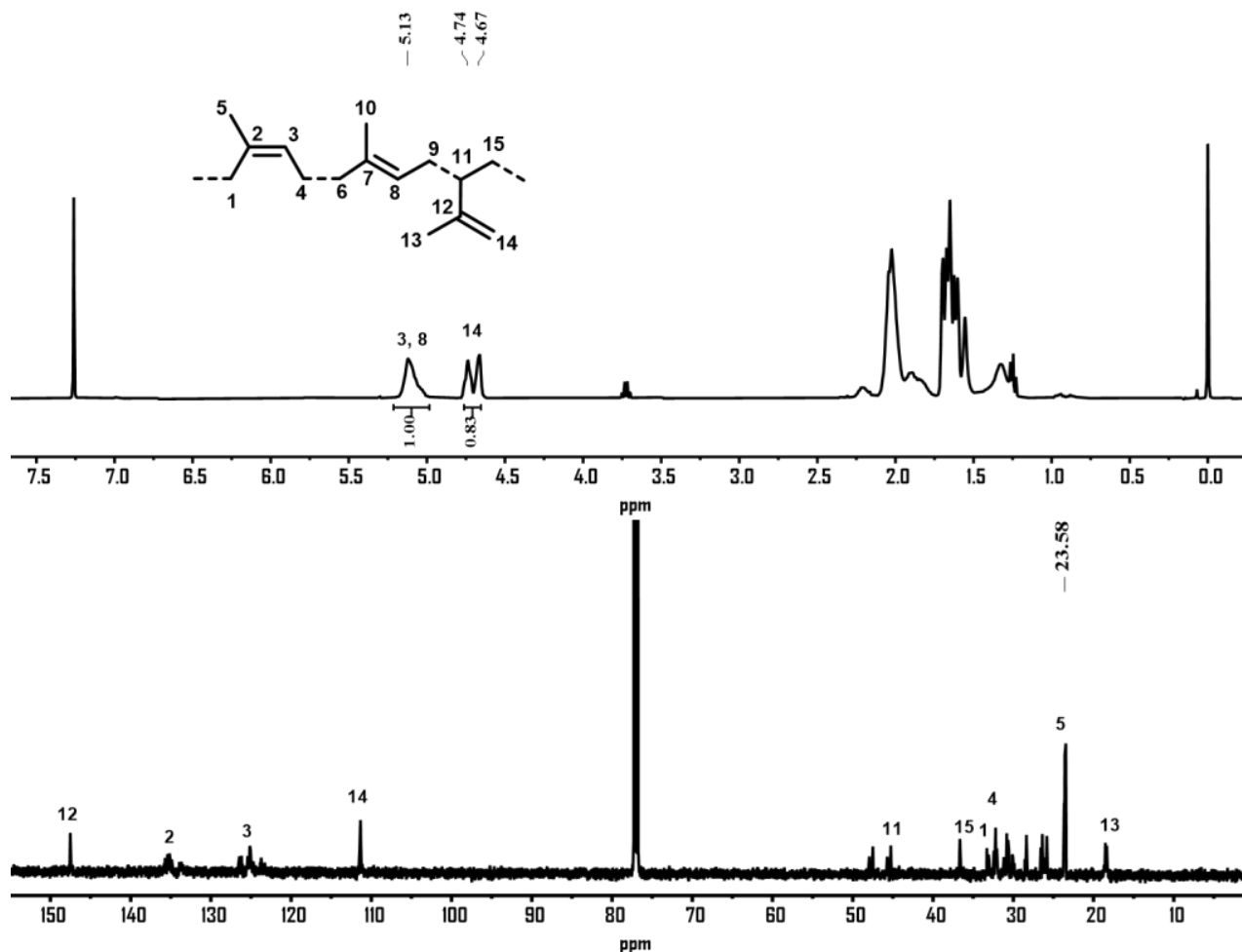
Subsequent isoprene polymerization experiments were carried out with varying Al/Co ratios ranging from 50 to 10 while maintaining a constant temperature of 25 °C for a duration of 1 h (entries 3–6, Table 2). Notably, a reduction in the Al/Co ratio from 50 to 40, and further down to 20, resulted in an improvement in polymerization activity, reaching a peak value of $0.4 \times 10^5 \text{ g (mol of Co)}^{-1}(\text{h})^{-1}$ at an Al/Co ratio of 20 (entry 5, Table 2). However, further decreasing the co-catalyst amount to 10 led to a decline in activity. This correlation between co-catalyst amount and polymerization activity aligns with previous findings in isoprene polymerization studies [17,23–25,33]. The increased concentration of the co-catalyst leads to a higher occurrence of chain transfer reactions, which was likely to result in the partial deactivation of the active species, ultimately leading to relatively lower yields when the co-catalyst concentration was high. At a monomer conversion of 22%, the resulting polyisoprene exhibited an average molecular weight (M_n) of $2.9 \times 10^5 \text{ g/mol}$, accompanied by a polydispersity index of 1.7. However, when the monomer conversion increased to 29% at an Al/Co ratio of 20 (entry 5, Table 2), a slightly lower M_n was observed. This discrepancy can be attributed to difficulty with polymer mass removal, as the presence of sticky polymer around the active species somehow hinders monomer insertion and increases the likelihood of chain transfer reactions, thus affecting chain propagation [17,23,45]. The microstructural features of polyisoprenes were analyzed using ^1H and ^{13}C NMR spectra [recorded in deuterated chloroform at room temperature], as shown in Figures S1–S18. The obtained spectra were compared with the literature to confirm the presence of characteristic peaks for *cis*-1,4 and *trans*-1,4 and 3,4 units [18,45]. Interestingly, there was no substantial influence on the selectivity of monomer insertion when varying the Al/Co ratios. The composition of 1,4 and 3,4 units remained almost consistent, with values ranging from 72% to 76% (consisting of both *cis*- and *trans*-1,4) and 24% to 28%, respectively, across all Al/Co ratios. The 1,4 monomer insertion is mainly *cis*-1,4 selectivity, accounting for 70% to 74% of overall composition of the resulting polyisoprene (entries 3–6, Table 2).

While the Al/Co ratio was maintained at the optimal value of 20, the temperature-dependent behavior of the polymerization reactions was investigated over a range of temperatures varying from 25 °C to 80 °C (entries 1–6, Table 3). The obtained results indicated a gradual increase in polymerization activity as the temperature was elevated, reaching complete conversion with the highest activity of $1.37 \times 10^5 \text{ g (mol of Co)}^{-1}(\text{h})^{-1}$ at 60 °C (entry 4, Table 3), resulting polyisoprene with high *cis*-1,4 selectivity (72%, confirmed from Figure 2). However, further elevation of the reaction temperature to 70 °C and above resulted in a consistent decline in polymerization activity. This decrease can be attributed to either partial decomposition of active species or formation of inactive species at higher temperatures, thus leading to reduced polymerization yields [16,17,20,35,45]. Despite the decrease in polymerization activity with increasing temperature, the catalytic system still displayed a remarkable activity of $1.12 \times 10^5 \text{ g (mol of Co)}^{-1}(\text{h})^{-1}$ with 82% conversion at 80 °C (entry 6, Table 3), demonstrating the excellent thermal stability of the prepared catalyst [29,35]. The molecular weight of the resulting polyisoprene gradually decreased with increasing reaction temperature up to 50 °C. It is presumed that elevated temperatures enhance the rate of chain transfer reactions and termination in comparison to chain propagation, thereby leading to a reduction in the molecular weights of the resulting polymers [17,23,45]. However, further increasing reaction temperature did not show a consistent change in molecular weight. This observation implies that the polymer yields at elevated temperature of 60 to 80 °C were in the range of 82% to over 99%; it is likely that this large amount of polymer surrounding the active species might impede chain transfer reactions, which in turn produces comparatively higher molecular weight polyisoprene [23,29]. Meanwhile, the influence of the reaction temperature on the selectivity of monomer insertion was not substantial. Increasing the reaction temperature led to a slight increase in 3,4 selectivity from 24% to 33%. In contrast, the selectivity of *cis*-1,4 monomer insertion showed minimal change, ranging from 66% to 73% (entries 1–6, Table 3). Similar findings have been reported in previous studies [16,17,20,24,34].

Table 3. Optimization of reaction conditions for isoprene polymerization using Co1 as the precatalyst ^a.

Entry	Temp. (°C)	Time (min)	Conv. (%) ^b	Act. ^c	M_n^d (10^5 g/mol)	PDI ^d	Microstructure ^e		
							<i>cis</i> -1,4	<i>trans</i> -1,4	3,4
1	25	60	29	0.40	2.8	1.6	71	5	24
2	40	60	35	0.48	2.2	2.0	73	2	25
3	50	60	59	0.80	1.4	2.3	73	1	26
4	60	60	>99	1.37	2.6	3.2	72	1	27
5	70	60	88	1.20	4.5	2.5	67	1	32
6	80	60	82	1.12	3.4	2.2	66	1	33
7	60	5	57	0.78	3.2	2.1	65	1	34
8	60	15	66	0.90	3.8	2.1	65	2	34
9	60	30	70	0.95	3.3	2.3	65	1	34
10	60	45	79	1.08	2.1	2.2	71	1	28
11 ^f	60	60	53	1.44	1.5	3.8	65	2	33
12 ^g	60	60	47	2.56	2.1	2.8	65	3	32

^a General conditions: catalyst Co1 (10 μ mol); co-catalyst AlMe₂Cl, Al/Co = 20, isoprene 2 mL (20 mmol), 5 mL toluene; ^b isolated yield; ^c 10^5 g (mol of Co)⁻¹(h)⁻¹; ^d determined by GPC, ^e selectivity given in mol%, determined by ¹H and ¹³C NMR spectra, ^f Co1 (5 μ mol), ^g Co1 (2.5 μ mol).

**Figure 2.** ¹H and ¹³C NMR spectra of the representative sample of polyisoprene obtained using Co1/AlMe₂Cl (Table 3, entry 4).

Next, the reaction running time was varied from 5 min to 60 min with the Al/Co ratio and temperature fixed at 20 and 60 °C respectively (entries 4 and 7–10, Table 3). It was observed that the polymerization activity and monomer conversion exhibited an almost

linear increase with the prolongation of reaction time (entries 4 and 7–10, Table 3), suggesting the long life of active species and a somewhat living behavior in promoting isoprene polymerization [33]. The molecular weights of the resulting polymer initially increased with the prolongation of reaction time up to 15 min, however, further prolonging the reaction time resulted in a decrease in molecular weights. Once again, this can be ascribed to the accumulation of a significant amount of polymer around the active species with longer reaction times, which likely hinders monomer insertion and leads to slightly lower molecular weights [17,23,45]. The selectivity of monomer insertion remained relatively consistent across all reaction running times, with *cis*-1,4 and 3,4 units ranging from 65% to 72% and 27% to 34%, respectively (entry 4 and 7–10, Table 3).

Finally, the effect of catalyst loading was investigated under optimal conditions (entries 11–12, Table 3). It was found that using a catalyst loading of 5 μmol resulted in 53% conversion, which is approximately half of the conversion achieved with a 10 μmol catalyst loading, while the activities remained relatively similar for both catalyst loadings (entry 4 vs. 11, Table 3). On the other hand, employing a catalyst loading of 2.5 μmol yielded a similar conversion compared to the 5 μmol catalyst loading, but significantly higher polymerization activity of $2.56 \times 10^5 \text{ g (mol of Co)}^{-1}(\text{h})^{-1}$ was obtained (entry 12, Table 3).

2.2.2. Isoprene Polymerization Using Complexes Co1–Co6

To investigate the impact of catalyst structure on the polymerization activity and properties of the resulting polyisoprene, besides Co1, the catalytic performance of all the complexes Co2–Co6 was examined for isoprene polymerization, and the results are presented in Table 4. The polymerization reactions were carried out under specific conditions, using toluene (5 mL) as solvent, with an IP/Co ratio of 2000, at 60 °C for a run time of 60 min. The results demonstrated that both electronic and steric substituents had a significant influence on the polymerization activity and the properties of the resulting polymer. The polymerization activities and isolated yields exhibited a decrease with increasing steric hindrance at the ortho position of the N-phenyl group (Figure 3) [33,34,36]. Among the complexes tested, the complex Co1, bearing the smallest steric groups (2,6-Me₂Ph), stands out as the top performer, providing the highest activity of $1.37 \times 10^5 \text{ g (mol of Co)}^{-1}(\text{h})^{-1}$ with a quantitative yield (entry 1, Table 4). The complex Co2 (2,6-Et₂Ph) and Co3 (2,6-*i*Pr₂Ph) followed in terms of activity, while Co6 (2,4,6-*t*Bu₃Ph), with the bulkiest steric groups, displayed the lowest polymerization activity. This suggests that the sterically bulky substituents at the ortho positions of the N-phenyl groups occupy more space around the active species. As a result, insertion and coordination of monomers were hindered at certain level, leading to relatively lower yields in the polymerization process [20,21].

Table 4. Isoprene polymerization by using Co1–Co6 ^a.

Entry	Cat.	Conv. (%) ^b	Act. ^c	M_n ^d (10^5)	PDI ^d	Microstructure ^e		
						<i>cis</i> -1,4	<i>trans</i> -1,4	3,4
1	Co1	>99	1.37	2.6	3.2	72	1	27
2	Co2	98	1.34	2.4	2.3	65	1	34
3	Co3	90	1.23	2.8	2.7	68	1	31
4	Co4	96	1.30	3.1	1.9	69	1	30
5	Co5	94	1.28	3.3	1.7	67	1	32
6	Co6	82	1.12	3.4	2.3	69	1	30

^a General conditions: catalyst loading 10 μmol ; co-catalyst AlMe₂Cl, Al/Co = 20, isoprene 2 mL (20 mmol), 5 mL toluene, temperature 60 °C, reaction time 1 h; ^b isolated yield; ^c $10^5 \text{ g (mol of Co)}^{-1}(\text{h})^{-1}$; ^d determined by GPC, ^e selectivity given in mol%, determined by ¹H and ¹³C NMR spectra.

Furthermore, the introduction of electron-donating groups at the para position of the N-phenyl group had a negative effect on the polymerization activities. The complexes Co4 and Co5, for example, showed slightly lower polymerization activity and monomer conversion compared to complexes Co1 and Co2 (entries 1 and 2 vs. entries 4 and 5, respectively, Table 4). The positive electronic effect of the methyl groups re-

duced the Lewis character of the metal center, impeding monomer coordination to some extent [20,21]. As depicted in Figure 3, the overall trend of decreasing polymerization activity was as follows: **Co1** (2,6-Me₂Ph) > **Co2** (2,6-Et₂Ph) > **Co4** (2,4,6-Me₃Ph) > **Co5** (2,6-Et₂-4-MePh) > **Co3** (2,6-*i*Pr₂Ph) > **Co6** (2,4,6-*t*Bu₃Ph). Meanwhile, the observed trend in molecular weights of the resulting polymer aligns with the dependence on the catalyst structure: **Co6** (2,4,6-*t*Bu₃Ph) > **Co5** (2,6-Et₂-4-MePh) > **Co4** (2,4,6-Me₃Ph) > **Co3** (2,6-*i*Pr₂Ph) > **Co1** (2,6-Me₂Ph) > **Co2** (2,6-Et₂Ph), as shown in Figure 3 [20,34]. The complexes with bulky groups tended to produce polyisoprene with higher molecular weights. **Co6**, bearing significant steric hindrance (2,4,6-*t*Bu₃Ph), yielded polyisoprene with the highest molecular weight, up to 3.4×10^5 g/mol (entry 6, Table 4). The presence of substantial steric hindrance at the axial sites of the metal center, as seen in **Co6**, shields the active species from undergoing extensive chain transfer reactions and promotes chain propagation, resulting in comparatively higher molecular weight polyisoprene. The findings regarding the influence of steric hindrance on molecular weight are consistent with previous studies [20]. The microstructure of the resulting polymers was minimally affected by steric hindrance. Analysis of the ¹H and ¹³C NMR spectra revealed that all the complexes exhibited a preference for *cis*-1,4 selectivity in monomer insertion. The *cis*-1,4 units in the resulting polymer ranged from 65% to 72%, while the 3,4 units ranged from 27% to 34%. The polyisoprene derived from **Co1** consisted of *cis*-1,4 units at 72% and 3,4 units at 27% (Figure 2). As for **Co6**, polymer composed of *cis*-1,4 and 3,4- units at 69% and 30%, respectively (Figure 4). **Co6**, with its large steric hindrance, displayed a greater inclination towards 1,4 monomer insertion selectivity [36]. Based on the analysis of the polymer microstructure, a mechanism for monomer coordination and insertion into the growing polymer chain is proposed (Figure 5). The allyl-cobalt intermediate contains two reactive sites, C1 and C3. Insertion of the incoming monomer at C1 results in the formation of a 1,4 addition, whereas insertion at C3 leads to the formation of a 3,4 unit. From the experimental findings presented in Table 4, it is evident that the *cis*- η^4 and anti-allyl-cobalt intermediate were more favorable. As a result, the major product observed was *cis*-1,4 polyisoprene, with a minor amount of 3,4 polyisoprene. In contrast, the structure of the catalysts does not seem to support the *trans*- η^4 mode of coordination and syn allyl-cobalt intermediate, as a negligible quantity of *trans*-1,4 units was observed in the resulting polymer. Overall, these findings indicate that catalyst structure, specifically the presence of electronic and steric substituents, plays a crucial role in the polymerization activity, molecular weight, and microstructure of the resulting polyisoprene. Understanding these structure–activity relationships can contribute to the development of tailored catalysts for controlling and optimizing the properties of polyisoprene polymers.

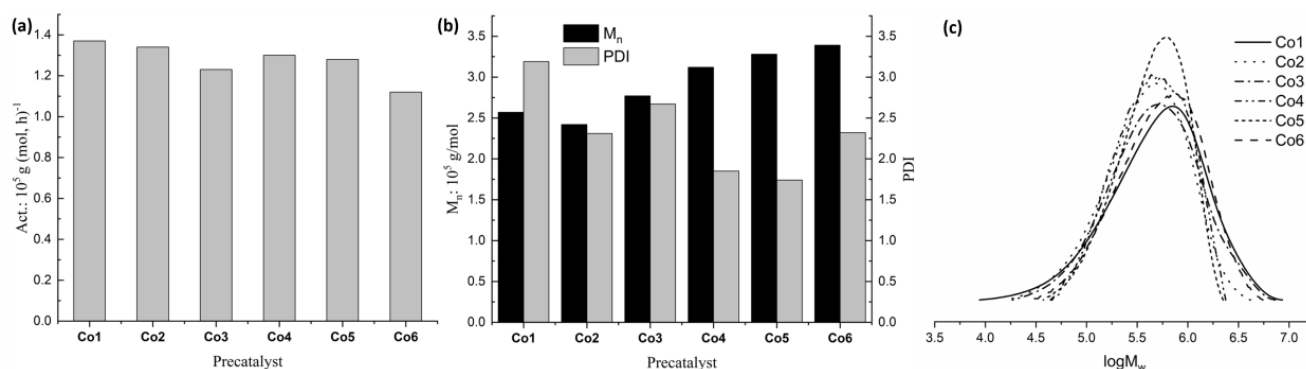


Figure 3. Polymerization activity (a), average molecular weight and molecular weight distribution (b), and GPC trace (c) for precatalysts **Co1–Co6**.

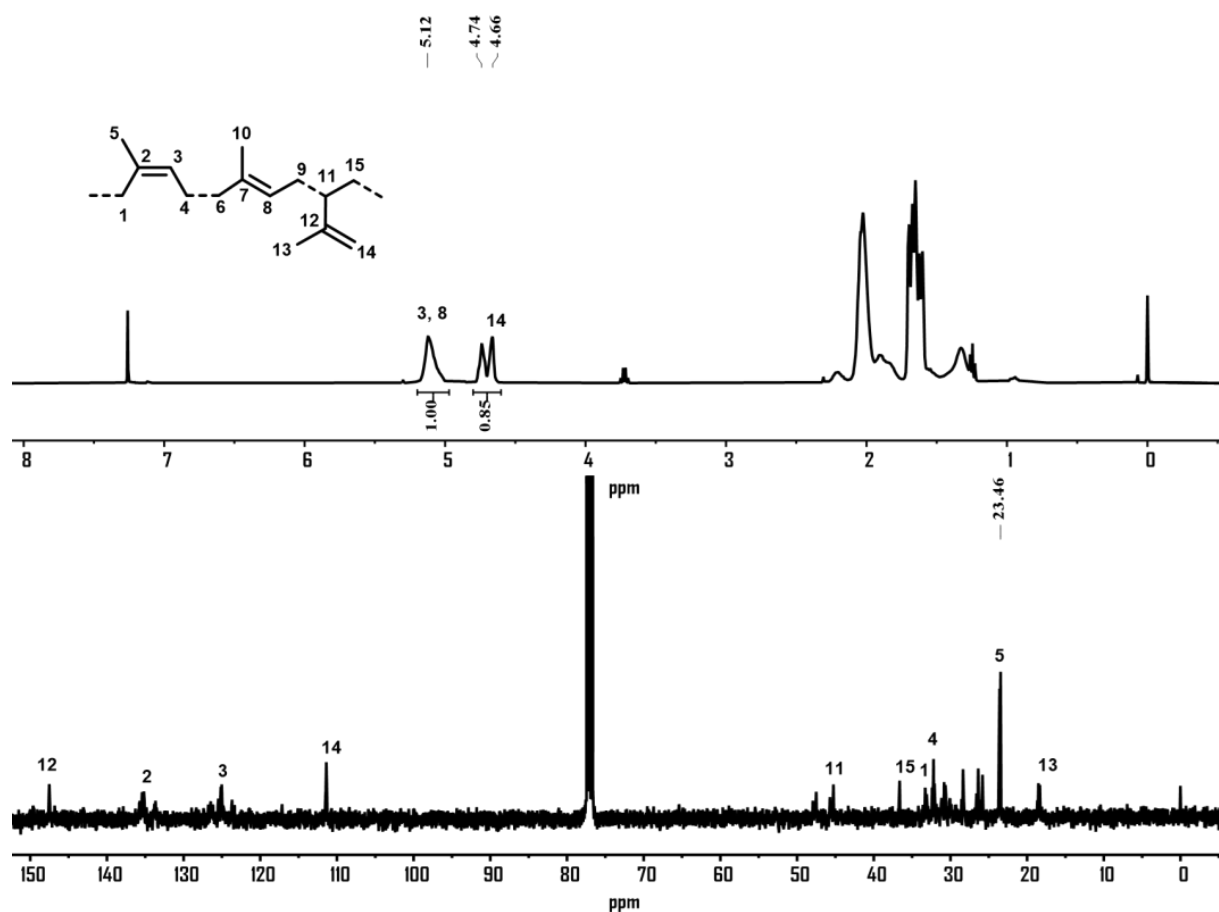


Figure 4. ^1H and ^{13}C NMR spectra of the representative sample of polyisoprene obtained using $\text{Co6}/\text{AlMe}_2\text{Cl}$ (Table 4, entry 6).

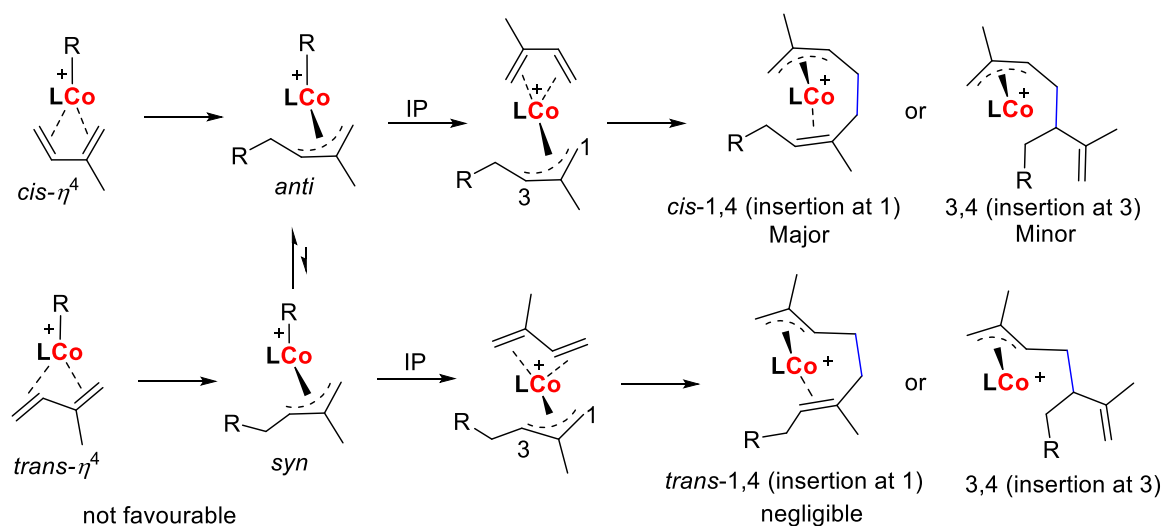


Figure 5. Possible mode of monomer coordination–insertion and corresponding polyisoprene configuration.

2.3. Comparison with Other Reported Iminopyridine Based Cobalt Complexes

Compared to the previously reported iminopyridine-cobalt complexes for isoprene polymerization, the newly synthesized cobalt complexes presented in this study exhibited comparable or better polymerization activity, molecular weights and monomer enchain-

ment selectivity. Under optimal conditions, the maximum polymerization activity achieved by the title complexes is $1.37 \times 10^5 \text{ g (mol of Co)}^{-1}(\text{h})^{-1}$, which is ten times higher than the activity reported for the complexes **A** [31] and **B** (chart) [32], but similar to that observed in complexes **C** (Chart 1) [33]. Moreover, the average molecular weights of the resulting polyisoprene were at the level of 10^5 g/mol , which are higher than the values of those obtained with complexes **A–C** in the Chart 1. It is worth noting that all the reported and prepared iminopyridine-cobalt complexes showed a preference for the *cis*-1,4 regioselectivity. In comparison to other bidentate cobalt complexes such as pyrazolyimine [24] and iminoimidazole-based cobalt complexes [25] reported elsewhere, the title complexes demonstrated superior polymerization activity and molecular weight of the resulting polyisoprene. Additionally, the title complexes also exhibited higher or comparable polymerization activity to the cobalt complexes bearing tridentate ligand structures [17,20,22,34,47]. However, the benefits of title complexes include their simple synthesis, use of less co-catalyst, and high molecular weight polyisoprene at the level of 10^5 g/mol .

3. Experimental Section

3.1. General Consideration and Materials

Manipulations of isoprene polymerization were typically conducted in an inert atmosphere of dry argon using standard Schlenk techniques or inside a glove box, and the synthesis of cobalt catalysts was performed in an open atmosphere. Toluene was dried using sodium metal, and all other solvents were refluxed over CaH_2 . Additionally, these solvents underwent distillation under an argon atmosphere prior to their use. The co-catalysts, namely MAO (1.67 M in toluene), AlMe_3 (2 M in toluene), and AlMe_2Cl (0.9 M in heptane), were purchased from Anhui Botai Electronic Materials Co., Chaoyang, China and Shanghai Macklin Biochemical Co., Ltd., Shanghai China, respectively, and used as received without any modifications. Isoprene of analytical grade was purchased from Beijing Yansan Petrochemical Co., purified via distillation over CaH_2 under an argon atmosphere, and stored at low temperature. All other commercially available chemicals were used without requiring additional purification. The ^1H and ^{13}C NMR measurements were conducted using a Bruker Ascend 400 MHz HD spectrometer (Ettlingen, Germany). All tests were performed at room temperature, and deuterated chloroform served as the internal standard. The chemical shifts are reported in ppm, and J values are reported in Hz. Fourier transform infrared (FT-IR) analysis was carried out using a PerkinElmer System 2000 FT-IR spectrometer, Waltham, MA, USA. The elemental composition of complexes was determined using a Flash EA 1112 micro-analyzer. Gel permeation chromatography (GPC) was performed using a PL-GPC50 instrument equipped (Agilent, Santa Clara, CA, USA) with a refractive index detector. The GPC system utilized mixed columns with a combined length of 650 and an internal diameter of 7.5 mm. The samples were dissolved in tetrahydrofuran (THF) at a temperature of 40°C . The elution of THF occurred at a flow rate of 1.0 mL/min. The columns were calibrated using standard polystyrene samples.

3.2. Synthesis and Characterization of (8-(Arylimino)-5,6,7-trihydroquinolin-2-yl)methyl Acetate-Cobalt Dichloride Complexes (**Co1–Co6**)

3.2.1. Aryl = 2,6- $\text{Me}_2\text{C}_6\text{H}_3$ (**Co1**)

General procedure: 2-(chloromethyl)-6,7-dihydroquinolin-8(5H)-one (100 mg, 0.5 mmol), $\text{CoCl}_2 \cdot 6\text{H}_2\text{O}$ (107 mg, 0.45 mmol), and an excess amount of 2,6-dimethylaniline (91 mg, 0.75 mmol) were added to acetic acid (5 mL) and heated to reflux with constant magnetic stirring. After 7 h of reaction time, all the volatiles were removed via low pressure, and the resulting crude product was redissolved in 2 mL dichloromethane. Subsequently, diethyl ether (5 mL) and *n*-hexane (20 mL) were added sequentially to generate the precipitates, and the resulting product was further washed with *n*-hexane and dried under vacuum to yield a green powder. Green solid, 335 mg, 74% yield. FT-IR (cm^{-1}): 3330.91 (m), 3215.29 (m), 2917.97 (m), 1746 (s), 1621.65 (s), 1586.56 (s), 1511.19 (m), 1473.83 (s), 1414.31 (m), 1362.58 (s),

1316.31 (m), 1141.94 (m), 1108.03 (w), 1048.16 (s), 838.60 (w), 770.04 (s). Anal. Calcd. for $C_{20}H_{22}Cl_2CoN_2O_2[5CH_2Cl_2]$: C, 34.24; H, 3.68; N, 3.19. Found: C, 33.97; H, 3.73; N, 3.56.

3.2.2. Aryl = 2,6-Et₂C₆H₃ (Co2)

Following a similar procedure as described for the synthesis of **Co1**, **Co2** was obtained as green solid (310 mg, 65% yield). FT-IR (cm⁻¹): 3232.18 (m), 3039.95 (w), 2919.09 (w), 2854.67 (w), 1745, 1646.8 (s), 1603.04 (m), 1537.84 (s), 1484.33 (s), 1432.05 (s), 1370.88 (s), 11313.38 (m), 1288.96 (s), 1226.30 (w), 1037.61 (w), 1014.17 (w), 859.17 (w), 739.33 (w), 715.82. Anal. Calcd. for $C_{22}H_{26}Cl_2CoN_2O_2$: C, 55.02; H, 5.46; N, 5.83. Found: C, 55.61; H, 5.48; N, 5.89.

3.2.3. Aryl = 2,6-iPr₂C₆H₃ (Co3)

Following a similar procedure as described for the synthesis of **Co1**, **Co3** was obtained as green solid (350 mg, 69% yield). FT-IR (cm⁻¹): 3551.11 (m), 3399.65 (m), 2962.10 (s), 2868.12 (w), 1747 (s), 1619 (m), 1587.53 (s), 1515.70 (w), 1472.07 (s), 1383.40 (w), 1325.92 (w), 1297.18 (w), 1184.47 (w), 1142.55 (w), 1109.96 (w), 1025.38 (w), 929.05 (w), 838.90 (w), 803.15 (m), 775.34 (s). Anal. Calcd. for $C_{24}H_{30}Cl_2CoN_2O_2[3CH_2Cl_2, Et_2O]$: C, 47.90; H, 5.90; N, 3.72. Found: C, 47.56; H, 5.36; N, 4.05.

3.2.4. Aryl = 2,4,6-Me₃C₆H₂ (Co4)

Following a similar procedure as described for the synthesis of **Co1**, **Co4** was obtained as green solid (335 mg, 72% yield). FT-IR (cm⁻¹): 3232.18 (m), 3039.95 (w), 2919.09 (w), 2854.67 (w), 1750 (s), 1646.8 (s), 1603.04 (m), 1537.84 (s), 1484.33 (s), 1432.05 (s), 1370.88 (s), 11313.38 (m), 1288.96 (s), 1226.30 (w), 1037.61 (w), 1014.17 (w), 859.17 (w), 739.33 (w), 715.82. Anal. Calcd. for $C_{21}H_{24}Cl_2CoN_2O_2$: C, 54.10; H, 5.19; N, 6.01. Found: C, 53.87; H, 5.24; N, 6.62.

3.2.5. Aryl = 2,6-Et₂-4-MeC₆H₂ (Co5)

Following a similar procedure as described for the synthesis of **Co1**, **Co5** was obtained as green solid (330 mg, 67% yield). FT-IR (cm⁻¹): 3367.04 (w), 2965.18 (m), 2932.57 (m), 2873.76 (m), 1744 (s), 1619.59 (m), 1589.66 (s), 1514.07 (m), 1457.29 (m), 1371.42 (s), 1221.77 (s), 1142.86 (m), 1101.90 (w), 1050.89 (s), 858.26 (s), 826.53 (w), 749.60 (w). Anal. Calcd. for $C_{23}H_{28}Cl_2CoN_2O_2[MeOH]$: C, 54.77; H, 6.13; N, 5.32. Found: C, 54.74; H, 6.23; N, 5.48.

3.2.6. Aryl = 2,4,6-tBu₃C₆H₂ (Co6)

Following a similar procedure as described for the synthesis of **Co1**, **Co6** was obtained as green solid (380 mg, 64% yield). FT-IR (cm⁻¹): 3400.41 (s), 2957.84 (s), 2868.79 (m), 1744.53 (m), 1621.44 (s), 1592.96 (s), 1516.21 (w), 1485.62 (m), 141431 (m), 1434.76 (w), 1393.84 (w), 1364.40 (m), 1220.77 (s), 1107.66 (m), 1086.07 (w), 1050.46 (m), 927.87 (w), 890.20 (w), 837.81 (w), 746.44 (w). Anal. Calcd. for $C_{30}H_{42}Cl_2CoN_2O_2[3CH_2Cl_2, H_2O]$: C, 45.81; H, 5.82; N, 3.24. Found: C, 45.81; H, 5.75; N, 3.69.

3.3. Polymerization Procedure

Under an inert argon atmosphere, a Schlenk flask was dried under reduced pressure and then filled with argon gas. While a flow of argon was maintained, the precatalysts such as **Co1** (10 μmol), toluene (5 mL) were added sequentially into this flask, followed by the addition of the assumed AlMe₂Cl. The resulting solution was stirred at the desired temperature for 1 min, and then isoprene (2 mL) was immediately injected. After the desired running time, the reaction was quenched by adding an acidic ethanol solution (ethanol/HCl = 50/1). The resulting polymer was washed with excess ethanol several times, filtered, and dried under vacuum at room temperature until no change was observed in weight.

3.4. X-ray Crystallographic Studies

The single-crystal X-ray diffraction analysis of **Co1** and **Co5** complexes was conducted using a Rigaku Sealed Tube CCD (Saturn 724+) diffractometer, Rigaku, Tokyo, Japan. The

diffractometer employed graphite-monochromated Cu-K α radiation with a wavelength (λ) of 0.71073 Å. The measurements were performed at a temperature of 170 (± 10) K. The cell parameters were determined by globally refining the positions of all collected reflections. The intensities obtained from the X-ray diffraction analysis were corrected for Lorentz and polymerization effects; an empirical absorption correction was carried out as well. The structures of complexes **Co1** and **Co5** were identified via direct methods and further refined via full-matrix least squares fitting on F2. The non-hydrogen atoms in each complex were refined anisotropically. The positions of all hydrogen atoms were determined based on calculated positions. The structural solution and refinement for each complex were carried out using SHELXT (Sheldrick) software. The solvent molecules, which do not influence the geometry of the main compound, were also processed using SHELXT [48]. The crystal data and processing parameters for **Co1** (CCDC 2270716) and **Co5** (CCDC 2270717) are presented in Table 5.

Table 5. Crystal data and structure refinement for **Co1** and **Co5** complexes.

	Co1	Co5
Identification code	2270716	2270717
Empirical formula	C ₂₀ H ₂₂ Cl ₂ CoN ₂ O ₂	C ₂₃ H ₂₈ Cl ₂ CoN ₂ O ₂
Formula weight	452.24	494.32
Temperature/K	169.98 (10)	169.99 (10)
Crystal system	monoclinic	triclinic
Space group	P2 ₁ /n	P-1
a/Å	9.1464 (4)	9.1668 (3)
b/Å	22.0899 (15)	10.4116 (4)
c/Å	10.6237 (4)	13.8557 (5)
α /°	90	71.220 (3)
β /°	106.870 (5)	87.520 (3)
γ /°	90	69.207 (3)
Volume/Å ³	2054.08 (19)	1166.68 (8)
Z	4	2
ρ calg/cm ³	1.462	1.419
μ /mm ⁻¹	9.048	8.024
F(000)	928.6	518.0
Crystal size/mm ³	0.15 × 0.10 × 0.05	0.15 × 0.10 × 0.05
Radiation	Cu K α (λ = 1.54184)	Cu K α (λ = 1.54184)
2 Θ range for data collection/	8.0 to 151.5 −11 ≤ h ≤ 11	6.8 to 151.5 −11 ≤ h ≤ 11
Index ranges	−25 ≤ k ≤ 27 −12 ≤ l ≤ 10	−13 ≤ k ≤ 12 −17 ≤ l ≤ 17
Reflections collected	17,017	13,334
Independent reflections	4097 [R _{int} = 0.0727, R _{sigma} = 0.0598]	4645 [R _{int} = 0.0441, R _{sigma} = 0.0430]
Data/restraints/parameters	4097/0/247	4645/1/282
Goodness-of-fit on F ²	1.032	1.040
Final R indexes [I > 2 σ (I)]	R ₁ = 0.0595, wR ₂ = 0.1508	R ₁ = 0.0636, wR ₂ = 0.1841
Final R indexes [all data]	R ₁ = 0.0914, wR ₂ = 0.1734	R ₁ = 0.0687, wR ₂ = 0.1884
Largest diff. peak/hole/e Å ⁻³	0.70/−0.72	1.07/−0.45

4. Conclusions

In this study, a series of well-defined cobalt complexes bearing the ligand framework of (8-(arylimino)-5,6,7-trihydroquinolin-2-yl)methyl acetate were designed, prepared, and thoroughly characterized via FT-IR, elemental analysis, and X-ray diffraction analysis in the cases of **Co1** and **Co5**. Interestingly, during the one-pot synthesis of these complexes, an unexpected substitution occurred, in which acetic acid, serving as the solvent, replaced a chloro group with an acetyl group, leading to the incorporation of a methyl

acetate moiety into the ligand structure. Among the tested catalyst systems, complex **Co1** combined with AlMe_2Cl resulted in a complete conversion with the highest activity of $1.37 \times 10^5 \text{ g (mol of Co)}^{-1}(\text{h})^{-1}$. Excellent thermal stability was observed, as the activity at 80°C could still preserve $1.12 \times 10^5 \text{ g (mol of Co)}^{-1}(\text{h})^{-1}$. The resulting polyisoprene possessed high molecular weight, ranging from 1.4 to $4.5 \times 10^5 \text{ g/mol}$ and exhibited a predominant presence of *cis*-1,4 units, ranging from 65% to 72%, while the 3,4 units accounted for 27% to 34% of the polymer structure. The structure–activity relationship analysis revealed that the introduction of steric substituents at the ortho position and electron-donating substituents at the para position of the N-aryl unit negatively affected catalytic activity. On the other hand, regarding the molecular weights of the resulting polyisoprene, an opposing trend was observed. Notably, the steric hindrance of the catalyst had minimal impact on this selectivity. Moreover, the presence of 3,4 units as pendant terminal olefin side chains in the resulting polyisoprene holds particular importance for post-modification of the polymer, as it offers the potential to modify and fine-tune the properties of the polymer. Overall, the designed cobalt complexes showed promising catalytic activity, control over the molecular weights, and selectivity for *cis*-1,4 units, providing insights for the synthesis and modification of polyisoprene polymers.

Supplementary Materials: The following supporting information can be downloaded at: <https://www.mdpi.com/article/10.3390/catal13071120/s1>. Figure S1. ^1H and ^{13}C NMR spectra of the polyisoprene obtained using **Co1**/ AlMe_2Cl (Table 2, entry 3), Figure S2. ^1H and ^{13}C NMR spectra of the polyisoprene obtained using **Co1**/ AlMe_2Cl (Table 2, entry 4), Figure S3. ^1H and ^{13}C NMR spectra of the polyisoprene obtained using **Co1**/ AlMe_2Cl (Table 2, entry 5), Figure S4. ^1H and ^{13}C NMR spectra of the polyisoprene obtained using **Co1**/ AlMe_2Cl (Table 2, entry 6). Figure S5. ^1H and ^{13}C NMR spectra of the polyisoprene obtained using **Co1**/ AlMe_2Cl (Table 3, entry 2), Figure S6. ^1H and ^{13}C NMR spectra of the polyisoprene obtained using **Co1**/ AlMe_2Cl (Table 3, entry 3), Figure S7. ^1H and ^{13}C NMR spectra of the polyisoprene obtained using **Co1**/ AlMe_2Cl (Table 3, entry 5), Figure S8. ^1H and ^{13}C NMR spectra of the polyisoprene obtained using **Co1**/ AlMe_2Cl (Table 3, entry 6), Figure S9. ^1H and ^{13}C NMR spectra of the polyisoprene obtained using **Co1**/ AlMe_2Cl (Table 3, entry 7), Figure S10. ^1H and ^{13}C NMR spectra of the polyisoprene obtained using **Co1**/ AlMe_2Cl (Table 3, entry 8), Figure S11. ^1H and ^{13}C NMR spectra of the polyisoprene obtained using **Co1**/ AlMe_2Cl (Table 3, entry 9), Figure S12. ^1H and ^{13}C NMR spectra of the polyisoprene obtained using **Co1**/ AlMe_2Cl (Table 3, entry 10), Figure S13. ^1H and ^{13}C NMR spectra of the polyisoprene obtained using **Co1**/ AlMe_2Cl (Table 3, entry 11), Figure S14. ^1H and ^{13}C NMR spectra of the polyisoprene obtained using **Co1**/ AlMe_2Cl (Table 3, entry 12), Figure S15. ^1H and ^{13}C NMR spectra of the polyisoprene obtained using **Co2**/ AlMe_2Cl (Table 4, entry 2), Figure S16. ^1H and ^{13}C NMR spectra of the polyisoprene obtained using **Co3**/ AlMe_2Cl (Table 4, entry 3), Figure S17. ^1H and ^{13}C NMR spectra of the polyisoprene obtained using **Co4**/ AlMe_2Cl (Table 4, entry 4), Figure S18. ^1H and ^{13}C NMR spectra of the polyisoprene obtained using **Co5**/ AlMe_2Cl (Table 4, entry 5).

Author Contributions: Conceptualization and data curation, W.-H.S., Q.M., Y.M., W.Z. and N.Y.; methodology, N.Y., R.Y. and Q.M.; synthesis of the organic compounds and polymers, N.Y.; characterization, N.Y., W.Z. and M.L.; investigation, N.Y., M.L. and R.Y.; writing—review and editing, N.Y., Y.M., Q.M. and W.-H.S.; project administration, W.-H.S. All authors have read and agreed to the published version of the manuscript.

Funding: This work has been financially supported by the Chemistry and Chemical Engineering Guangdong Laboratory (No. 2111018 and 2132012).

Data Availability Statement: Data will be made available by the corresponding author upon request.

Acknowledgments: N.Y. thanks the Chinese Government Scholarship-Belt and Road Program and the ANSO Scholarship for financial support.

Conflicts of Interest: There are no conflicts of interests.

References

1. Li, D.; Li, S.; Cui, D.; Zhang, X. β -Diketiminato rare-earth metal complexes: Structures, catalysis, and active species for highly *cis*-1,4-selective polymerization of isoprene. *Organometallics* **2010**, *29*, 2186–2193. [CrossRef]
2. Ouaddad, S.; Bakleh, M.E.; Kostjuk, S.V.; Ganachaud, F.; Puskas, J.E.; Deffieux, A.; Peruch, F. Bio-inspired cationic polymerization of isoprene and analogues: State-of-the-art. *Polym. Int.* **2012**, *61*, 149–156. [CrossRef]
3. Ricci, G.; Pampaloni, G.; Sommazzi, A.; Masi, F. Dienes polymerization: Where we are and what lies ahead. *Macromolecules* **2021**, *54*, 5879–5914. [CrossRef]
4. Ricci, G.; Sommazzi, A.; Masi, F.; Ricci, M.; Boglia, A.; Leone, G. Well-defined transition metal complexes with phosphorus and nitrogen ligands for 1,3-dienes polymerization. *Coord. Chem. Rev.* **2010**, *254*, 661–676. [CrossRef]
5. Song, J.S.; Huang, B.C.; Yu, D.S. Progress of synthesis and application of *trans*-1,4-polyisoprene. *J. Appl. Polym. Sci.* **2001**, *82*, 81–89. [CrossRef]
6. Nakajima, N. *Science and Practice of Rubber Mixing*; Rapra Technology Ltd.: Shawbury, Shropshire, UK, 2000.
7. Friebe, L.; Nuyken, O.; Obrecht, W. Neodymium-Based ziegler/natta catalysts and their application in diene polymerization. *Adv. Polym. Sci.* **2006**, *204*, 1–154.
8. Wang, B.; Cui, D.; Lv, K. Highly 3,4-selective living polymerization of isoprene with rare earth metal fluorenyl N-heterocyclic carbene precursors. *Macromolecules* **2008**, *41*, 1983–1988. [CrossRef]
9. Liu, H.; He, J.; Liu, Z.; Lin, Z.; Du, G.; Zhang, S.; Li, X. Quasi-living *trans*-1,4-polymerization of isoprene by cationic rare earth metal alkyl species bearing a chiral (S,S)-bis(oxazolinyphenyl)amido ligand. *Macromolecules* **2013**, *46*, 3257–3265. [CrossRef]
10. Jia, A.Q.; Wang, J.Q.; Hu, P.; Jin, G.X. Syntheses, reactions, and ethylene polymerization of titanium complexes with [N,N,S] ligands. *Dalton Trans.* **2011**, *40*, 7730–7736. [CrossRef]
11. Johnson, L.K.; Killian, C.M.; Brookhart, M. New Pd(II)- and Ni(II)-based catalysts for polymerization of ethylene and α -olefins. *J. Am. Chem. Soc.* **1995**, *117*, 6414–6415. [CrossRef]
12. Killian, C.M.; Tempel, D.J.; Johnson, L.K.; Brookhart, M. Living polymerization of α -olefins using Ni(II)- α -diimine catalysts. synthesis of new block polymers based on α -olefins. *J. Am. Chem. Soc.* **1996**, *118*, 11664–11665. [CrossRef]
13. Small, B.L.; Brookhart, M.; Bennett, A.M.A. Highly active iron and cobalt catalysts for the polymerization of ethylene. *J. Am. Chem. Soc.* **1998**, *120*, 4049–4050. [CrossRef]
14. Britovsek, G.J.P.; Gibson, V.C.; Kimberley, B.S.; Maddox, P.J.; McTavish, S.J.; Solan, G.A.; White, A.J.P.; Williams, D.J. Novel olefin polymerization catalysts based on iron and cobalt. *Chem. Commun.* **1998**, *7*, 849–850. [CrossRef]
15. Champouret, Y.; Hashmi, O.H.; Visseaux, M. Discrete iron-based complexes: Applications in homogeneous coordination-insertion polymerization catalysis. *Coord. Chem. Rev.* **2019**, *390*, 127–170. [CrossRef]
16. Alnajrani, M.N.; Mair, F.S. Bidentate forms of β -triketimines: Syntheses, characterization and outstanding performance of enamine-diimine cobalt complexes in isoprene polymerization. *Dalton Trans.* **2016**, *45*, 10435–10446. [CrossRef]
17. Zhao, J.; Chen, H.; Li, W.; Jia, X.; Zhang, X.; Gong, D. Polymerization of isoprene promoted by aminophosphine(ory)-fused bipyridine cobalt complexes: Precise control of molecular weight and *cis*-1,4-alt-3,4 Sequence. *Inorg. Chem.* **2018**, *57*, 4088–4097. [CrossRef]
18. Raynaud, J.; Wu, J.Y.; Ritter, T. Iron-catalyzed polymerization of isoprene and other 1,3-Dienes. *Angew. Chem. Int. Ed.* **2012**, *51*, 11805–11808. [CrossRef] [PubMed]
19. Wang, L.; Wang, X.; Hou, H.; Zhu, G.; Han, Z.; Yang, W.; Chen, X.; Wang, Q. An unsymmetrical binuclear iminopyridine-iron complex and its catalytic isoprene polymerization. *Chem. Commun.* **2020**, *56*, 8846–8849. [CrossRef]
20. Fang, L.; Zhao, W.; Han, C.; Liu, H.; Hu, Y.; Zhang, X. Isoprene polymerization with pyrazolyimine cobalt (II) complexes: Manipulation 3,4-selectivities by ligand design and triphenyl phosphine. *Eur. J. Inorg. Chem.* **2019**, *2019*, 609–616. [CrossRef]
21. Zhang, X.; Zhu, G.; Mahmood, Q.; Zhao, M.; Wang, L.; Jing, C.; Wang, X.; Wang, Q. Iminoimidazole-based Co(II) and Fe(II) complexes: Syntheses, characterization, and catalytic behaviors for isoprene polymerization. *J. Polym. Sci. PART A Polym. Chem.* **2019**, *57*, 767–775. [CrossRef]
22. Zhao, M.; Ma, Y.; Zhang, X.; Wang, L.; Zhu, G.; Wang, Q. Synthesis, characterization and catalytic property studies for isoprene polymerization of iron complexes bearing unionized pyridine-oxime ligands. *Polymers* **2022**, *14*, 3612. [CrossRef]
23. Wang, G.; Jiang, X.; Zhao, W.; Sun, W.-H.; Yao, W.; He, A. Catalytic behavior of Co(II) complexes with 2-(Benzimidazolyl)-6-(1-(arylimino)ethyl)pyridine ligands on isoprene stereospecific polymerization. *J. Appl. Polym. Sci.* **2013**, *131*, 1. [CrossRef]
24. Jiang, X.; Wen, X.; Sun, W.-H.; He, A. Polymerization of isoprene catalyzed by 2-(Methyl-2 benzimidazolyl)-6-(1-(arylimino) ethyl) Pyridine Iron(III) trichloride with an additional donor. *J. Polym. Sci. PART A Polym. Chem.* **2014**, *52*, 2395–2398. [CrossRef]
25. He, A.; Wang, G.; Zhao, W.; Jiang, X.; Yao, W.; Sun, W.-H. High *cis*-1,4 polyisoprene or *cis*-1,4/3,4 binary polyisoprene synthesized using 2-(benzimidazolyl)-6-(1-(arylimino)ethyl)pyridine cobalt(II) dichlorides. *Polym. Int.* **2013**, *62*, 1758–1766. [CrossRef]
26. Alnajrani, M.N.; Mair, F.S. The behaviour of β -triketimine cobalt complexes in the polymerization of isoprene. *RSC Adv.* **2015**, *5*, 46372–46385. [CrossRef]
27. Zhao, M.; Wang, L.; Mahmood, Q.; Jing, C.; Zhu, G.; Zhang, X.; Wang, X.; Wang, Q. Controlled isoprene polymerization mediated by iminopyridine-iron (II) acetylacetonate pre-catalysts. *Appl. Organometal. Chem.* **2019**, *33*, e4836. [CrossRef]
28. Hashmi, O.H.; Champouret, Y.; Visseaux, M. Highly active iminopyridyl iron-based catalysts for the polymerization of isoprene. *Molecules* **2019**, *24*, 3024. [CrossRef] [PubMed]

29. Zhu, G.; Wang, L.; Mahmood, Q.; Zhou, L.; Wang, Q. Ligand-regulated polymerization of conjugated dienes catalyzed by confined iminopyridine iron complexes with high activity and thermal stability. *Polym. Test.* **2021**, *102*, 107317. [[CrossRef](#)]
30. Ricci, G.; Leone, G.; Zanchin, G.; Palucci, B.; Boccia, A.C.; Sommazzi, A.; Masi, F.; Zacchini, S.; Guelfi, M.; Pampaloni, G. Highly stereoregular 1,3-butadiene and isoprene polymers through monoalkyl-N-aryl substituted iminopyridine iron complex-based catalysts: Synthesis and characterization. *Macromolecules* **2021**, *54*, 9947–9959. [[CrossRef](#)]
31. Guo, L.; Jing, X.; Xiong, S.; Liu, W.; Liu, Y.; Liu, Z.; Chen, C. Influences of alkyl and aryl substituents on iminopyridine Fe(II)- and Co(II)-catalyzed isoprene polymerization. *Polymers* **2016**, *8*, 389. [[CrossRef](#)]
32. Zhu, G.; Zhang, X.; Zhao, M.; Wang, L.; Jing, C.; Wang, P.; Wang, X.; Wang, Q. Influences of fluorine substituents on iminopyridine Fe(II)- and Co(II)-catalyzed isoprene polymerization. *Polymers* **2018**, *10*, 934. [[CrossRef](#)]
33. Lin, W.; Zhang, L.; Suo, H.; Vignesh, A.; Yousuf, N.; Hao, X.; Sun, W.-H. Synthesis of characteristic polyisoprenes using rationally designed iminopyridyl metal (Fe and Co) precatalysts: Investigation of co-catalysts and steric influence on their catalytic activity. *New J. Chem.* **2020**, *44*, 8076–8084. [[CrossRef](#)]
34. Wang, X.; Fan, L.; Huang, C.; Liang, T.; Guo, C.Y.; Sun, W.-H. Highly *cis*-1,4 selective polymerization of isoprene promoted by α -diimine cobalt(II) chlorides. *J. Polym. Sci. Part A Polym. Chem.* **2016**, *54*, 3609–3615. [[CrossRef](#)]
35. Jing, C.; Wang, L.; Zhu, G.; Hou, H.; Zhou, L.; Wang, Q. Enhancing thermal stability in aminopyridine iron(II)-catalyzed polymerization of conjugated dienes. *Organometallics* **2020**, *39*, 4019–4026. [[CrossRef](#)]
36. Zhao, M.; Zhang, X.; Wang, L.; Wang, L.; Zhu, G.; Wang, Q. Pyridine-oxazoline ligated iron complexes: Synthesis, characterization, and catalytic activity for isoprene polymerization. *Appl. Organomet. Chem.* **2022**, *36*, e6848. [[CrossRef](#)]
37. Yu, J.; Zeng, Y.; Huang, W.; Hao, X.; Sun, W.-H. N-(5,6,7-trihydroquinolin-8-ylidene)arylammonium nickel dichlorides as highly active single-site pro-catalysts in ethylene polymerization. *Dalton Trans.* **2011**, *40*, 8436–8443. [[CrossRef](#)] [[PubMed](#)]
38. Sun, Z.; Yue, E.; Qu, M.; Oleynik, I.V.; Oleynik, I.I.; Li, K.; Liang, T.; Zhang, W.; Sun, W.-H. 8-(2-cycloalkylphenylimino)-5,6,7-trihydroquinolynickel halides: Polymerizing ethylene to highly branched and lower molecular weight polyethylenes. *Inorg. Chem. Front.* **2015**, *2*, 223–227. [[CrossRef](#)]
39. Guo, J.; Zhang, W.; Mahmood, Q.; Zhang, R.; Sun, Y.; Sun, W.-H. Vinyl/vinylene functionalized highly Branched polyethylene waxes obtained using electronically controlled cyclohexyl-fused pyridinylimine-nickel precatalysts. *J. Polym. Sci. PART A Polym. Chem.* **2018**, *56*, 1269–1281. [[CrossRef](#)]
40. Li, J.; Zhang, Q.; Hu, X.; Ma, Y.; Solan, G.A.; Sun, Y.; Sun, W.-H. 2-Acetyloxymethyl-substituted 5,6,7-trihydroquinolynyl-8-ylideneamine-Ni(II) chlorides and their application in ethylene dimerization/trimerization. *Appl. Organomet. Chem.* **2019**, *34*, e5254. [[CrossRef](#)]
41. Jiang, S.; Zheng, Y.; Liu, M.; Yu, Z.; Ma, Y.; Solan, G.A.; Zhang, W.; Liang, T.; Sun, W.-H. Polyethylene waxes with short chain branching via steric and electronic tuning of an 8-(arylimino)-5,6,7-trihydroquinoline-nickel catalyst. *Organometallics* **2022**, *41*, 3197–3211. [[CrossRef](#)]
42. Lin, W.; Liu, M.; Xu, L.; Ma, Y.; Zhang, L.; Flisak, Z.; Hu, X.; Liang, T.; Sun, W.-H. Nickel(II) complexes with sterically hindered 5,6,7-trihydroquinoline derivatives selectively dimerizing ethylene to 1-butene. *Appl. Organomet. Chem.* **2022**, *36*, e6596. [[CrossRef](#)]
43. Xua, L.; Li, J.; Lin, W.; Ma, Y.; Hua, X.; Flisak, Z.; Sun, W.-H. Ethylene oligomerization with 2-hydroxymethyl-5,6,7-trihydroquinolynyl-8-ylideneamine-Ni(II) chlorides. *J. Organomet. Chem.* **2021**, *937*, 121720. [[CrossRef](#)]
44. Hou, X.; Cai, Z.; Chen, X.; Wang, L.; Redshaw, C.; Sun, W.-H. N-(5,6,7-trihydroquinolin-8-ylidene)-2-benzhydrylbenzenaminonickel halide complexes: Synthesis, characterization and catalytic behavior towards ethylene polymerization. *Dalton Trans.* **2012**, *41*, 1617–1623. [[CrossRef](#)] [[PubMed](#)]
45. Jing, C.; Wang, L.; Mahmood, Q.; Zhao, M.; Zhu, G.; Zhang, X.; Wang, X.; Wang, Q. Synthesis and characterization of aminopyridine iron(II) chloride catalysts for isoprene polymerization: Sterically controlled monomer enchainment. *Dalton Trans.* **2019**, *48*, 7862–7874. [[CrossRef](#)]
46. Zhang, L.; Hao, X.; Sun, W.-H.; Redshaw, C. Synthesis, characterization, and ethylene polymerization behavior of 8-(nitroarylamino)-5,6,7-trihydroquinolynickel dichlorides: Influence of the nitro group and impurities on catalytic activity liping. *ACS Catal.* **2011**, *1*, 1213–1220. [[CrossRef](#)]
47. Bonnet, F.; Dyer, H.E.; Kinani, Y.E.; Dietz, C.; Roussel, P.; Bria, M.; Viseaux, M.; Zinck, P.; Mountford, P. Bis(phenolate)amine-supported lanthanide borohydride complexes for styrene and *trans*-1,4-isoprene (co-)polymerisations. *Dalton Trans.* **2015**, *44*, 12312–12325. [[CrossRef](#)] [[PubMed](#)]
48. Sheldrick, G.M. *SHELXTL-97, Program for the Refinement of Crystal Structures*; University of Göttingen: Göttingen, Germany, 1997.

Disclaimer/Publisher's Note: The statements, opinions and data contained in all publications are solely those of the individual author(s) and contributor(s) and not of MDPI and/or the editor(s). MDPI and/or the editor(s) disclaim responsibility for any injury to people or property resulting from any ideas, methods, instructions or products referred to in the content.